Nonplanar Effects on Pitch-Plane Dynamics

L. E. Ericsson*
Lockheed Missiles & Space Company, Inc., Sunnyvale, California
and
M. E. Beyers†
National Aeronautical Establishment, Ottawa, Ontario, Canada

A new interpretation of the free-flight data of a sharp 10-deg cone and a blunt 60-deg cone is presented. A reassessment of the analysis of the original data is made, and an appropriate nonplanar motion correlator is derived. It is shown that nonplanar motion effects are the probable cause of the observed anomalous motions. In the case of the 10-deg cone, the principal nonplanar flow mechanism is the coning-induced tilting of forebody vortices; in the case of the 60-deg cone, the principal mechanism is the coupling between body motion and the near-wake recirculation region, possibly amplified by test-related effects.

Nomenclature

a	= speed of sound
C_{mj}	= pitching-moment derivative with respect to the reduced-rate parameter, $[\partial C_m/\partial(jd/2U_\infty)]$, $j=p,q,\dot{\alpha},\dot{\sigma},\dot{\phi}$
$C_{mq}+C_{m\dot{\alpha}}$	= pitch damping derivative
d	= base diameter
I	= moment of inertia; subscripts x, y, and z refer to moments of inertia about the body axes x, y, and z
K_1,K_2,K_3	= tricyclic vectors
l	= distance aft of model base
L	= distance aft of c.g., $L=x-x_{c.g.}$
M	= Mach number
m	= pitching moment, coefficient $C_m=m/(\rho_\infty U_\infty^2/2)Sd$
NPR	= nonplanar ratio, see Eq. (1)
p	= roll rate
q	= pitch rate
S	= reference area, $=\pi d^2/4$
t	= time
U_∞	= freestream velocity
U	= convection velocity
V	= velocity relative to tunnel reference, positive upstream
X	= independent variable, distance flown
x,y,z	= body axes
$x_{c.g.}$	= center-of-mass location, aft of nose
α,β	= aeroballistic angles of attack and sideslip
γ	= tilt angle of vortex system off symmetry plane (Fig.6)
Δ	= increment or amplitude
ϵ	= mass offset
ρ	= air density
σ	= total angle of attack, $=\tan^{-1}[(\tan^2\alpha+\tan^2\beta)^{1/2}]$
σ_0	= trim value of σ
$\bar{\sigma}^2$	= mean-square resultant angle of attack for flight
φ	= Euler roll angle
ϕ	= rotation of pitch plane
ϕ_1,ϕ_2,ϕ_3	= tricyclic vector angles
ϕ_1',ϕ_2'	= tricyclic vector rates
ψ	= phase angle, $=\omega t$
ω	= circular frequency

Subscripts

d	= downstream
f	= final
ff	= free flight
m	= model launch
p	= platform
s	= separation from sting flare or launcher
u	= upstream
w	= wake neck
0	= initial and/or reference condition
∞	= freestream condition

Superscripts

$(')$	= differentiation with respect to X
$(\cdot)$	= differentiation with respect to t
$(*)$	= effective, constant fixed-axis derivative
$(\bar{\ })$	= mean value

Presented as Paper 88-0215 at the AIAA 26th Aerospace Sciences Meeting, Reno, NV, Jan. 11-14, 1988; received Sept. 12, 1988; revision received April 14, 1989.

*Senior Consulting Engineer. Fellow AIAA.
†Senior Research Officer. Member AIAA.

Introduction

AN experimental program was conducted in the late 1960s by Jaffe[1] to investigate the differences between nonplanar and planar stability derivatives of bodies of revolution in free flight. Two widely different configurations, a sharp 10-deg half-angle cone and a blunted 60-deg cone, were studied using the wind-tunnel free-flight technique. When analyzing the test data, Jaffe noticed a phase shift between tricyclic predictions and the nonplanar free-flight data. These systematic deviations in the α-β motions could be documented clearly by virtue of the high degree of refinement in Jaffe's experiment[1] (Fig. 1). After scrutinizing several sources of experimental error, Jaffe concluded that the phase shift was a consequence of nonlinear characteristics caused by the physical flow, not represented in the theoretical force model.

Subsequently, several other researchers entered the debate,[2-7] introducing somewhat ambiguous interpretations of the observed phenomenon. Chapman,[3] for instance, first included a series of nonlinear static terms and then utilized the mathematical model due to Tobak et al.,[5] and Tobak and Schiff,[6] but could not fully account for the phase shift. Beyers[7] analyzed the tricyclic residuals, showing that the

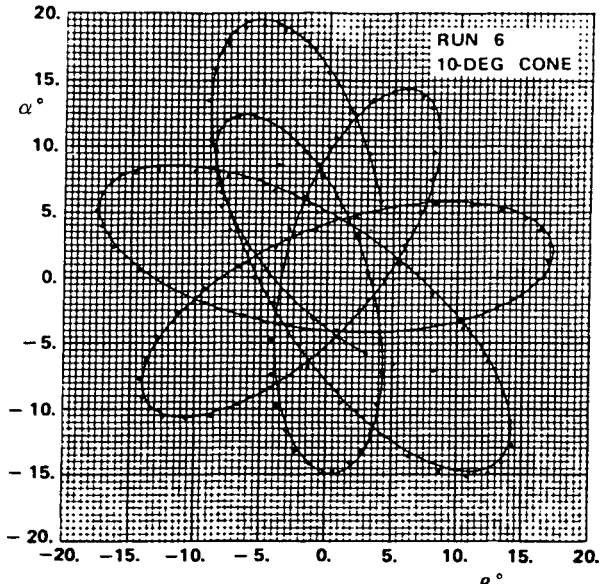

a. 10° cone

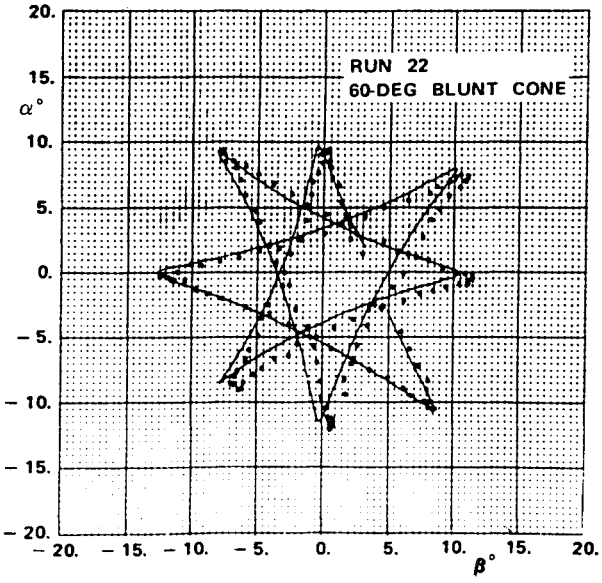

b. 60° blunt cone

Fig. 1 Typical α-β plots.[1]

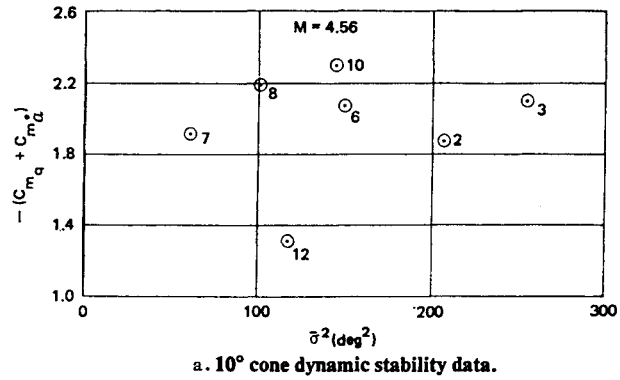

a. 10° cone dynamic stability data.

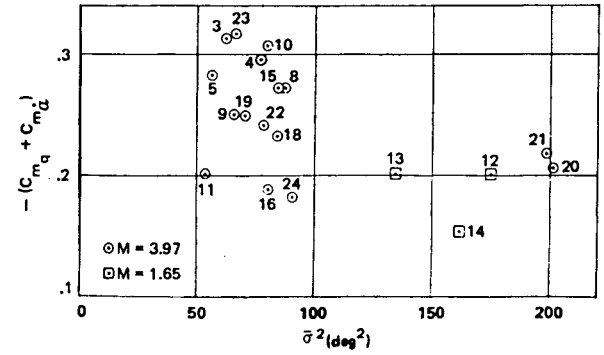

b. 60° blunt cone dynamic stability data.

Fig. 2 Correlation of dynamic stability data as a function of $\bar\sigma^2$.[1]

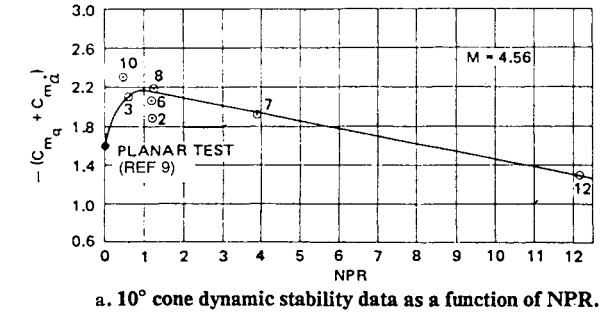

a. 10° cone dynamic stability data as a function of NPR.

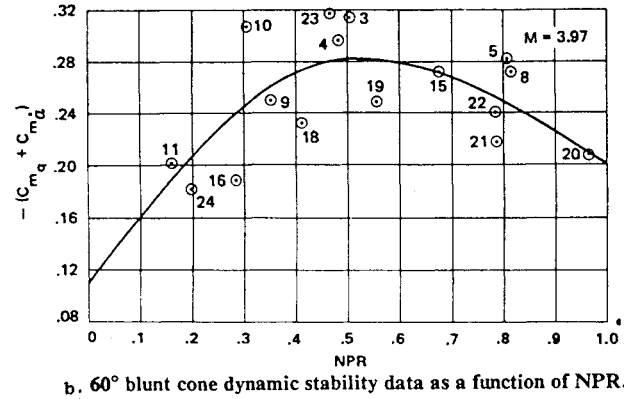

b. 60° blunt cone dynamic stability data as a function of NPR.

Fig. 3 Correlation of dynamic stability data as a function of NPR.[1]

phase shift was consistent with the combined effects of asymmetrical products of inertia and a nonlinear pitching moment, but the result was again inconclusive.

In this paper, the viscous flow mechanisms that could result in such angular phase lags are discussed, and the nonplanar motion effect on the measured pitch damping is analyzed. Subsequently, the analysis of the free-flight motion is reassessed, and the effect of launcher interference is considered.

Nonplanar Flow Mechanics

When the measured pitch-damping derivative was plotted as a function of the mean-square resultant angle of attack $\bar\sigma^2$, the results did not show the expected correlation (Fig. 2). Following a suggestion based on the results obtained by Tobak et al.,[5] Jaffe[1] introduced the coning rate to formulate a nonplanar ratio, NPR, which appeared to serve well as a correlation parameter (Fig. 3). Jaffe's conclusion: "The dynamic stability results show the same trend for both configurations: a sharp favorable increase in the coefficient as the motion becomes slightly nonplanar, and then a constant decrease as the motion becomes more nonplanar."[1]

Jaffe[1] defined this nonplanar ratio as follows (see Fig. 4).

$$\mathrm{NPR}=\int_{X_0}^{X_f}|\sigma\phi'|\,dX\Big/\int_{X_0}^{X_f}|\sigma'|\,dX \qquad (1)$$

Following the approach used to define an effective damping derivative that represents what is measured in a wind-tunnel test, where an additional degree of freedom often is introduced by sting plunging and the aerodynamics are highly

nonlinear,[8] one can define the effective pitch damping in the presence of out-of-plane motion as

$$C^*_{m\dot{\sigma}\dot{\phi}}\int \frac{l\dot{\sigma}}{U_\infty}\,d\sigma = \int C_{m\dot{\sigma}}\frac{l\dot{\sigma}}{U_\infty}\,d\sigma + \int C_{m\dot{\phi}}\frac{l\sigma\dot{\phi}}{U_\infty}\,d\phi \qquad (2)$$

The nonlinearity can be eliminated by representing the integrated effects of $C_{m\dot{\sigma}}$ and $C_{m\dot{\phi}}$ by the effective constant derivatives $C^*_{m\dot{\sigma}}$ and $C^*_{m\dot{\phi}}$. Substituting $d\sigma=\sigma'\,dX$, $d\phi=\phi'\,dX$, and $\dot{\sigma}=\sigma' U_\infty$, $\dot{\phi}=\phi' U_\infty$ in Eq. (2), the nonplanar motion effect can be expressed as

$$C^*_{m\dot{\sigma}\dot{\phi}} = C^*_{m\dot{\sigma}} + C^*_{m\dot{\phi}}\left(\int_{t_0}^{t_f}\sigma\phi'^2 dX \Big/ \int_{t_0}^{t_f}\sigma'^2 dX\right) \qquad (3)$$

Comparing Eqs. (1) and (3), one can see that there is a significant difference. To specify this further, Eq. (2) will be evaluated in the time domain, writing $d\sigma=\dot{\sigma}\,dt$ and $d\phi=\dot{\phi}\,dt$. The result is

$$C^*_{m\dot{\sigma}\dot{\phi}} = C^*_{m\dot{\sigma}} + C^*_{m\dot{\phi}}\left(\int_{t_0}^{t_f}\sigma\dot{\phi}^2\,dt \Big/ \int_{t_0}^{t_f}\dot{\sigma}^2\,dt\right) \qquad (4)$$

With $\sigma=\sigma_0+\Delta\sigma\sin\psi$, where $\psi=\omega t$, Eq. (4) can be written as

$$C^*_{m\dot{\sigma}\dot{\phi}} = C^*_{m\dot{\sigma}} + C^*_{m\dot{\phi}} \times\left[\int_{\psi_0}^{\psi_f}\dot{\phi}^2(\sigma_0+\Delta\sigma\sin\psi)\,d\psi \Big/ \int_{\psi_0}^{\psi_f}(\Delta\sigma\omega)^2\cos^2\psi\,d\psi\right] \qquad (5)$$

It is the integrated mean magnitude $|\dot{\sigma}|$ of the pitch rate that is of interest. Assuming that σ_0 and $\Delta\sigma$ remain constant, as well as ω and $|\dot{\phi}|$, for each half-cycle, one obtains the effect of the out-of-plane motion by looking at all of the "upstroke" and "downstroke" pitch half-cycles individually and taking the mean. For one upstroke half-cycle, $\psi_0=-\pi/2$ and $\psi_f=\pi/2$ in Eq. (5). Thus, one obtains

$$C^*_{m\dot{\sigma}\dot{\phi}} = C^*_{m\dot{\sigma}} + C^*_{m\dot{\phi}}(\dot{\phi}/\dot{\sigma})^2(4/\pi)[(\pi/2)\sigma_0+\Delta\sigma] \qquad (6)$$

Evaluating Eq. (1) in the same manner gives

$$\mathrm{NPR} = (|\dot{\phi}|/|\dot{\sigma}|)[(\pi/2)\sigma_0+\Delta\sigma] \qquad (7)$$

Thus, Eq. (6) can be expressed as follows, using NPR as defined by Eq. (7).

$$C^*_{m\dot{\sigma}\dot{\phi}} = C^*_{m\dot{\sigma}} + C^*_{m\dot{\phi}}(4/\pi)(\mathrm{NPR})^2/[(\pi/2)\sigma_0+\Delta\sigma] \qquad (8)$$

The same equation is obtained when taking the mean of several half-cycles. That is, $(\mathrm{NPR})^2$ rather than NPR is the correct correlation parameter for the nonplanar motion effect. Replotting Fig. 3 as a function of $(\mathrm{NPR})^2$ gives the results shown in Fig. 5. For the 10-deg cone, the measured damping derivative from a previous planar free-flight test[9] obviously does not give any relevant information. It really did not either when using NPR as a correlation parameter (Fig. 3). One data trend emerges, however, in both Figs. 3 and 5—the pitch damping decreases as the out-of-plane motion increases. The deviation from that data trend for $(\mathrm{NPR})^2<0.1$ for the 60-deg cone in Fig. 5b needs to be investigated further.

In regard to the data trend for the 10-deg cone, the majority of the results are for $\sigma\geq 10$ deg (see Fig. 2). Consequently, symmetric body vortices, starting at the pointed nose, will be present,[10] even at high supersonic speeds.[11] From the studies by Tobak et al.[5] and Schiff and Tobak,[12] one can construct the flow picture shown in Fig. 6. That is, the symmetric vortex pair is tilted at an angle γ off of the centerline, along the full

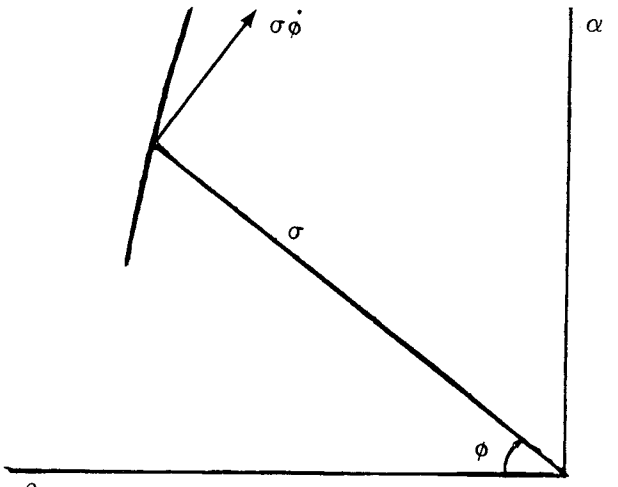

Fig. 4 Definition of angular coordinates.

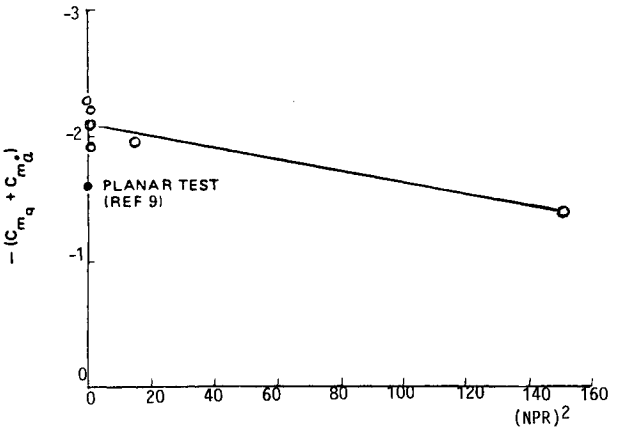

a. 10° cone dynamic stability data as a function of $(\mathrm{NPR})^2$

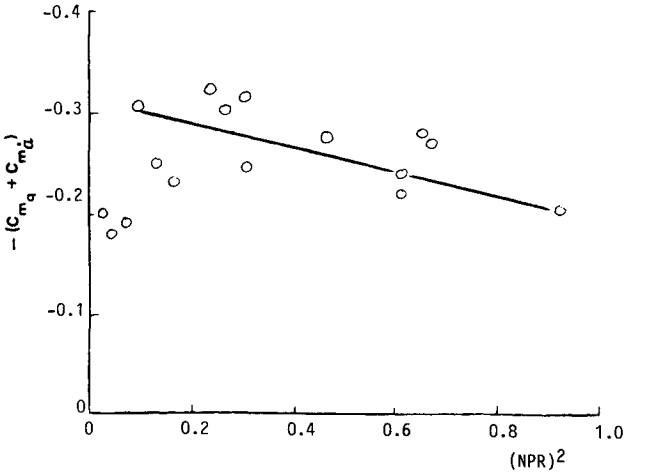

b. 60° blunt cone dynamic stability data as a function of $(\mathrm{NPR})^2$

Fig. 5 Correlation of dynamic stability data as a function of $(\mathrm{NPR})^2$.

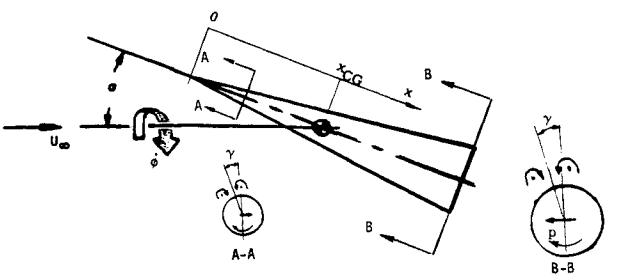

Fig. 6 Slender-cone vortex geometry.

length of the cone, where

$$\tan\gamma = x_{c.g.}\dot{\phi}/U_\infty \tag{9}$$

Forward of the center of mass the vortex-induced effect will resist the coning motion; aft of c.g. it will drive it. The latter effect will dominate because of the combined effect of increasing cross-sectional area and lever arm for the load induced aft of the c.g. The resulting coning-rate increase will cause the motion lobes in Fig. 1a to widen. Consequently, the portion of the oscillation cycle for which symmetric vortices are present, at $\sigma \geq 10$ deg, will increase.

Thus, a negative damping contribution that increases with increasing coning rate is generated by the symmetric vortex pair. In addition to the tilting of the symmetric vortex pair through an angle γ, there is the so-called moving-wall effect,[13] which will act on the two vortices individually, generated by both the coning and spinning motions. To determine to what extent these moving-wall effects influence the nonplanar motion is beyond the scope of the present paper.

In regard to the observed phase lag between experimental results and tricyclic predictions (Fig. 1), it should be noted that, for the 10-deg cone, there is a downstream convective time lag associated with the vortex-induced load[14]; for the 60-deg blunt cone, the base pressure reaction to the base recirculation process is associated with an upstream convective time lag of a much larger magnitude.[15] Not accounting for time-lag effects could be the explanation for the observed phase lags between experiment and prediction, with the 60-deg blunt cone showing the largest effect.[1]

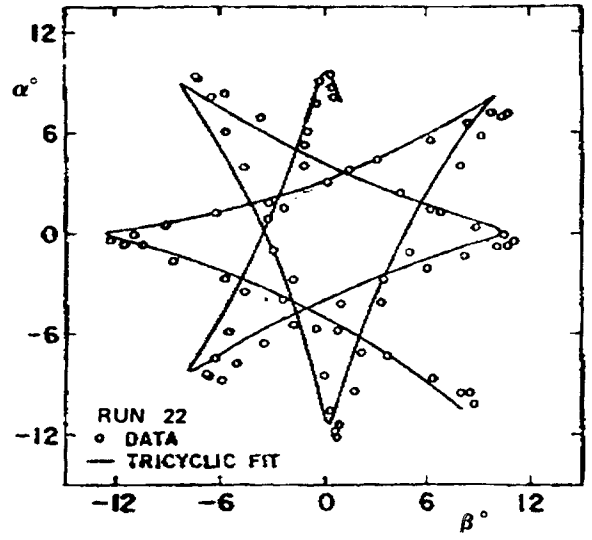

a. Linear fit

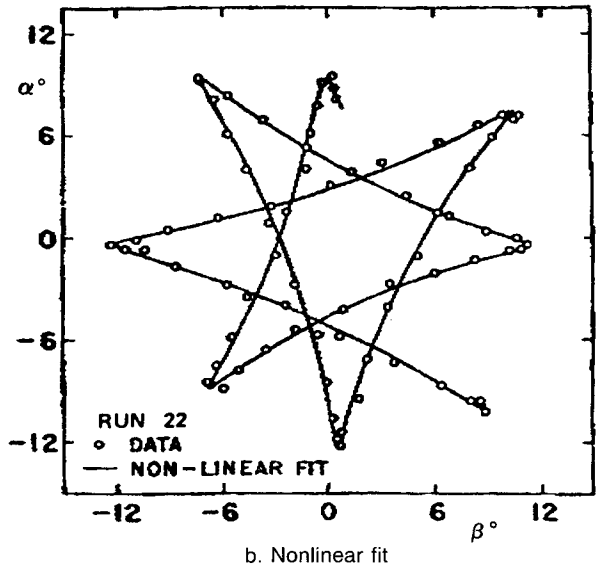

b. Nonlinear fit

Fig. 7 Tricyclic fits of 6-DOF simulated flight data for 60-deg cone.[7]

Free-Flight Motion Analysis

A reassessment of the analysis of the Jet Propulsion Laboratory (JPL) free-flight data records[1] can now be made. The data were processed by curve fitting the angular data with the tricyclic equation[16]

$$\sin\beta + i\sin\alpha = K_1 e^{i\phi_1} + K_2 e^{i\phi_2} + K_3 e^{i\phi_3} \tag{10}$$

Normally, 10 constants, or 9 if the roll rate is known, are determined in the differential-correction, curve-fitting process, defining the initial conditions, trim angle, roll rate, and the derivatives $C_{m\alpha}$, $C_{mq} + C_{m\dot{\alpha}}$, and $C_{mp\alpha}$. To account for the variation in p/U_∞ due to deceleration, as well as for a cubic pitching moment, Jaffe also used a 12-constant fit.[1] The additional unknowns arise from the ϕ'' terms in an expansion of the vector rates

$$\phi_{1,2} = (\phi_{1,2})_0 + \phi'_{1,2}X + (\tfrac{1}{2})\phi''_{1,2}X^2 \tag{11}$$

The additional constants substantially improved the fit for a six-degree-of-freedom (DOF) simulation of one of the blunt-body flights (run 21) but, as might be expected, did not completely account for the phase shift in the actual flights; a systematic deviation in the residuals remained. For run 22, for example, the rms deviation decreased from 0.8 deg (Fig. 1 or

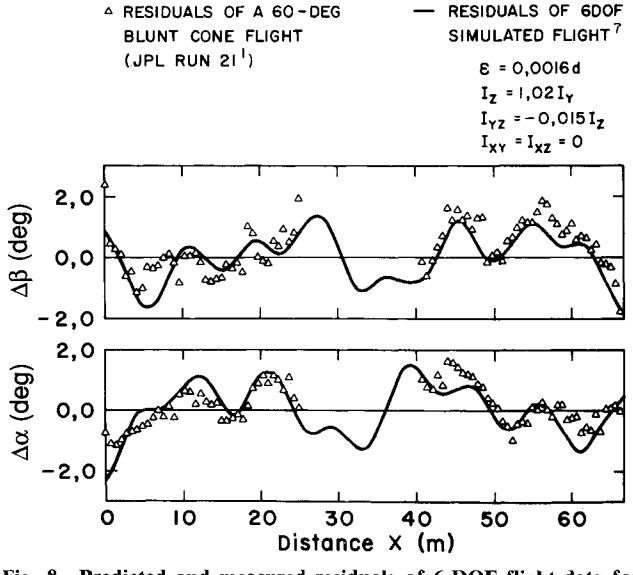

Fig. 8 Predicted and measured residuals of 6-DOF flight data for 60-deg cone.[7]

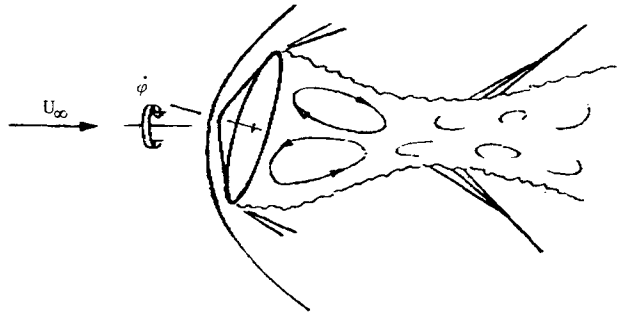

Fig. 9 Blunt cone near-wake.

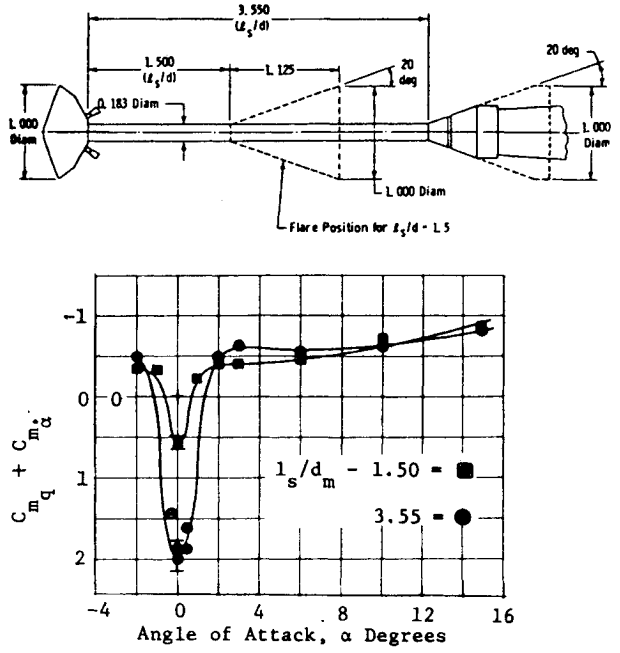

Fig. 10 Effect of sting support interference on measured damping of the Viking model.[18]

Fig. 7a) to 0.25 deg for the reconstructed data[17] depicted in Fig. 7b. In the motions in Figs. 7a and 7b, some data points have been omitted (see discussion under Test-Related Effects). Evidently, other effects are present in addition to the nonlinear pitching moment and p/U_∞ variation. The damping decrease with increasing coning rate, caused by the vortex displacement and augmented by moving-wall effects, will be accompanied by increasing coning and precession rates. This effect will be manifested as slowly varying tricyclic vector rates ϕ_1' and ϕ_2'.

Thus, the addition of two constants in the fitting process could account for the increasing precession rate due to nonplanar aerodynamic effects; this is consistent with Jaffe's finding that the 12-constant model improves the fit of the experimental data.[1] However, this increases the danger that the curve fit will account for non-flight-dynamic nonlinearities. A more satisfactory approach would be to revise the force model to include nonsymmetrical aerodynamics and aerodynamic cross-coupling moments.

The possibility of inertial cross coupling was studied in the inverse process, namely, through a 6-DOF simulation[7] of one of the blunt 60-deg cone flights (run 21), using the aerodynamic data and initial conditions obtained from the tricyclic fit of the wind-tunnel data.[1] From a comparison of the nonlinear components of the angular motion, contained in the residuals of tricyclic curve fits of the experimental and simulated flights (see Fig. 8), it was deduced[7] that a plausible asymmetric mass distribution with $I_{yz} = -0.015I_z$, combined with a bicubic pitching moment, could account for the systematic deviation. However, significant out-of-plane reactions associated with the large upstream convective time lags would be generated for a configuration of this type in coning motion (see Fig. 9). Thus, it now seems likely that inertial asymmetry was only part of the problem and that possibly equally large aerodynamic cross-coupling moments were present.

Aerodynamic Cross Coupling

Aerodynamic coupling can be generated in free flight by the near-wake recirculation effects discussed in Ref. 15. A convective time lag Δt_{ff} is associated with the communication of disturbances from the model down to the wake neck and back, at the mean convection velocities $\bar{U}_d$ and $\bar{U}_u$, respectively,

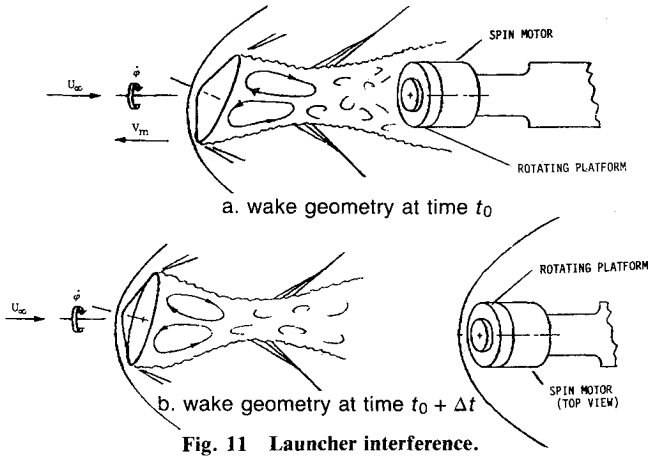

Fig. 11 Launcher interference.

where

$$\Delta t_{ff} = l_w[(1/\bar{U}_d) + (1/\bar{U}_u)] \tag{12}$$

The negative damping in pitch at $\alpha = 0$, measured at $M_\infty = 1.76$ on a model of the Viking probe[18] (Fig. 10), is the likely result of the phase lag generated by the time lag Δt, the negative damping being of an even larger magnitude in the absence of the support and its associated interference.[19] In the present case, during the time Δt the model rotates through the angle $\Delta\varphi$ (see Fig. 9), where

$$\Delta\varphi = \dot{\varphi}_0 \Delta t \tag{13}$$

For the Viking model (Fig. 10), the experimental results[18] gave a wake length $l_w \leq 2d$ for $M_\infty \geq 2$. According to Refs. 15 and 18, one can assume that $\bar{U}_d \approx 0.8U_\infty$ and $\bar{U}_u \approx 0.4a$. The blunt 60-deg cone model tested at $M_\infty = 3.97$, with a base diameter of $d = 1.5$ in. and an initial rotation rate of $\dot{\varphi}_0 \approx 35$ rev/s, would have a phase lag of $\Delta\varphi = 14$ deg according to Eqs. (12) and (13). In comparison, for the 10-deg sharp cone, with only downstream convection and $d = 1$ in., $M_\infty = 4.56$, $\bar{U}_d \approx U_\infty$, one obtains the phase lag $\Delta\varphi = 3$ deg for $\dot{\varphi}_0 = 135$ rev/s, a factor of 5 smaller than for the blunt 60-deg cone model. This is consistent with the large phase shifts observed in the 60-deg cone flights. Since the lagging reactions are out of plane, the pitch damping will decrease as $(NPR)^2$ increases (Fig. 5b). The apparent increase in damping with $(NPR)^2$ at small values of $(NPR)^2$ is the subject of further study.

Test-Related Effects

In analyzing the free-flight data, the fits were found to improve significantly when the first few data points were omitted.[17] In run 22, for instance, the standard deviation of the total angle σ for the 60-deg cone reduced from approximately 1 to 0.83 deg for a nine-constant fit when the first and last five data points were omitted (Fig. 7a). This raises the question whether the phase shift between the tricyclic fits and the data might not be due, in part, to test-related effects.

The release point for the gun-launched models was usually approximately 7 in. downstream of the edge of the window to insure that the wake is free of any influence from the launch head during the observable trajectory.[20] However, because of the severe launch velocity requirement for high-drag shapes, some of the 60-deg cone models could have been launched closer to the viewing area than 7 in., which corresponds to 4.7 d for the 60-deg blunt cone. For the first few frames of motion, the wake is wholly or partially obscured and cannot be examined on the film records; hence, the possibility of launcher interference must be considered. This is similar to dynamic support interference,[19] in that it is characterized by a convective time lag Δt, associated with the communication of disturbances within the subsonic wake region. In the present case, however, this is a more complex phenomenon because of the dynamic launch-induced forces and rotational effects for a coning or precessing model (see Fig. 11).

If l_s is the separation distance between the launcher platform and the model at time t_0, $\bar{V}_p$ the mean platform velocity, and $\bar{V}_s$ the mean separation velocity, the disturbance will have traveled from the model down to the launcher and back to the model base at time $t_0+\Delta t$. The distances traveled downstream and upstream are $l_s-\bar{V}_p\Delta t_d$ and $l_s+\bar{V}_s\Delta t$, respectively. Hence,

$$\Delta t=\frac{l_s-\bar{V}_p\Delta t_d}{\bar{U}_d}+\frac{l_s+\bar{V}_s\Delta t}{\bar{U}_u} \tag{14}$$

where $\Delta t_d\approx l_s/\bar{U}_d$ and the mean convection velocities $\bar{U}_d$ and $\bar{U}_u$ are measured relative to the wind-tunnel reference. Because of the recoil of the launcher piston at the end of its acceleration stroke, $\bar{V}_p$ is small and can be neglected in Eq. (14). Thus, the time lag becomes

$$\Delta t = l_s\left[(1/\bar{U}_d)+(1/\bar{U}_u)\right]/\left[1-(\bar{V}_s/\bar{U}_u)\right] \tag{15}$$

Strictly speaking, the separation velocity is variable due to the platform motion $V_p=V_p(t)$, and V_s becomes

$$V_s=\bar{V}_m-V_p(t) \tag{16}$$

Except at the time of the model release, V_p is small, $V_p\ll\bar{V}_m$. This was the case for the test discussed in Ref. 1, where the piston was decelerated by means of a deforming buffer system. thus,

$$\Delta t = l_s\left[(1/\bar{U}_d)+(1/\bar{U}_u)\right]/\left[1-(\bar{V}_m/\bar{U}_u)\right] \tag{17}$$

That is, with Eq. (12),

$$\Delta t = \Delta t_{\mathrm{ff}}(l_s/l_w)/[1-(\bar{V}_m/\bar{U}_u)] \tag{18}$$

When the launcher platform is located in the wake neck, i.e., $l_s=l_w$, the interference reaches its maximum.[15,19] With $\bar{U}_d$ and $\bar{U}_u$ the same as before and $\bar{V}_m/U_\infty=0.1$, Eq. (18) yields $\Delta t\to\infty$. For $\bar{V}_m/U_\infty=0.05$, Eqs. (13) and (18) give $\Delta\varphi=29$ deg for $\dot{\varphi}=35$ rev/s. Thus, large phase lags could be induced by launcher interference during the early stages of the model free flight. This phase lag would be much larger for the 60-deg cone than for the 10-deg cone. In the former case, the wake dimension l_w is approximately 50% larger and the launch velocity approximately three times higher.

In addition to the convective time-lag effect, direct interference from the launch platform will also occur during the model/launcher separation event. Initially, the model wake encloses the launcher platform. With increasing separation distance, the subsonic region is at some time cut off from the launcher, forming a closed near-wake region. The formation of a detached shock at the platform will cause a pressure pulse to be propagated upstream through the wake. Because of the large base area of the 60-deg cone and the dominant effect of base pressure on the vehicle aerodynamics, this pressure pulse could generate a strong base force perturbation, which, if not distributed evenly, could introduce an abrupt change in the coning and precessional angular velocities. This would cause a phase shift in the α-β diagram. As with the convective time-lag effect, this would be partially accounted for by variable vector rates, as in Eq. (11).

To minimize both the convective and impulsive interference effects, in more recent free-flight experiments the model was launched with a large vertical velocity component to obtain more rapid separation of the model wake from the launch platform.[21]

Measurements of the model attitude in the vicinity of the window trailing edge could contain bias errors not present further upstream. By virtue of its high-drag characteristics, the 60-deg cone enters and leaves the field of view at approximately three times the speed of the 10-deg cone. This would result in a much greater image distortion in the case of the 60-deg cone than for the 10-deg cone. The film reading error is exacerbated by the tapering biplanar field of view, which obscures one side of the image in the first and last few frames of motion.

Both continuous (convective time lag) and impulsive interference effects, as well as reading errors, would tend to contribute to the angular phase shift and, thereby, could affect the damping indirectly through a change in the decay mechanism. Being repeatable, these effects will be systematic and will, therefore, influence the data trends. However, the waveform distortion has a second-order effect on the damping. Thus, the observed data trends are primarily the result of the aerodynamic mechanisms described.

It should be emphasized that the sole purpose of the present analysis is to show how out-of-plane motion affects a scalar, planar measurement such as the pitch damping. As was alluded to in the text, in addition to the NPR parameter, one also has to consider the ratio of body spin to pitch rate. This parameter will be important when the moving-wall effects[13] are significant, as would especially be the case when the competing NPR parameter becomes small, e.g., for $(\mathrm{NPR})^2<0.1$ in Fig. 5b. A correct description of the vehicle motion characteristics can be achieved only by use of a method that accounts for the nonplanar, nonlinear character of the vehicle dynamics.[5,6]

Conclusions

The present analysis has shed new light on the longstanding question of the source of the phase shifts between free-flight motions and tricyclic curve fits originally obtained by Jaffe. The appropriate correlator for nonplanar motion effects was found to be the square of the ratio between the coning and pitching angular velocities. From the improved correlation of the measured pitch damping for the 10-deg cone with this parameter, it is evident that the phase shift is related to the coning rate. This effect on the damping is found to be the likely manifestation of aerodynamic cross-coupling moments due to coning-induced vortex asymmetry and moving-wall effects.

A similar correlation was found for the 60-deg cone, but the possibility that the accumulated effects of experimental bias could have contributed appreciably to the observed phase shift cannot be ruled out. However, except in the initial and final segments of the trajectories, these errors were probably small in view of the highly controlled nature of Jaffe's experiment. Therefore, the main component of the phase shift probably can be attributed to the effect on the response of aerodynamic and inertial cross coupling. At nonzero spin rate, the dominant effect is the aerodynamic cross coupling produced by the lagging out-of-plane reaction to base recirculation changes.

References

[1]Jaffe, P., "Nonplanar Tests Using the Wind-Tunnel Free-Flight Technique," *Journal of Spacecraft and Rockets*, Vol. 10, July 1973, pp. 435-442.

[2]Lusardi, R. J., "The Determination of Non-Symmetric Vehicle Stability Parameters from Response Data," Ph.D. Thesis, Univ. of Notre Dame, South Bend, IN, May 1973.

[3]Chapman, G. T., "Aerodynamic Parameter Identification in Ballistic Range Tests," *Proceedings of the 1972 Army Numerical Analysis Conference*, Edgewood Arsenal, Edgewood, MD, April 1972.

[4]Chapman, G. T. and Kirk, D. B., "Nonlinear Parameter Identification-Ballistic Range Experience Applicable to Flight Testing," *Parameter Estimation Techniques and Applications in Aircraft Flight Testing*, NASA TN D-7647, April 1974, pp. 191-195.

[5]Tobak, M., Schiff, L. B., and Peterson, V. L., "Aerodynamics of Bodies of Revolution in Coning Motion," *AIAA Journal*, Vol. 7, Jan. 1969, pp. 95-99.

[6]Tobak, M. and Schiff, L. B., "A Nonlinear Aerodynamic Moment Formulation and Its Implications for Dynamic Stability Testing," AIAA Paper 71-275, March 1971.

[7]Beyers, M. E., "Identification of Non-Linear Components of Free-Flight Motion," Atmospheric Flight Mechanics Workshop, AIAA Mechanics and Control of Flight Conference, Aug. 1974; also,

Council for Scientific and Industrial Research, Pretoria, South Africa, CSIR Rept. ME 1334, Aug. 1974.

[8]Ericsson, L. E., "Effect of Sting Plunging on Measured Nonlinear Pitching Damping," AIAA Paper 78-832, April 1978.

[9]Jaffe, P. and Prislin, R. H., "Effect of Boundary-Layer Transition on Dynamic Stability," *Journal of Spacecraft and Rockets*, Vol. 3, Jan. 1966, pp. 46-52.

[10]Ericsson, L. E. and Reding, J. P., "Asymmetric Vortex Shedding from Bodies of Revolution," *Tactical Missile Aerodynamics,* Progress in Astronautics and Aeronautics: Vol. 104, edited by M. J. Hemsch and J. N. Nielsen, 1986, Chap. 7, pp. 243-296.

[11]Rainbird, W. J., "The External Flow Field About Yawed Circular Cones," AGARD Meeting on Hypersonic Boundary Layers and Flow Fields, Paper 19, AGARD CP-30, London, May 1968.

[12]Schiff, L. B. and Tobak, M., "Results from a New Wind-Tunnel Apparatus for Studying Coning and Spinning Motions of Bodies of Revolution," *AIAA Journal*, Vol. 8, Nov. 1970, pp. 1953-1958.

[13]Ericsson, L. E., "Moving Wall Effects in Unsteady Flow," *Journal of Aircraft*, Vol. 25, Nov. 1988, pp. 977-990.

[14]Ericsson, L. E., Transition Effects on Slender Cone Pitch Damping," *Journal of Spacecraft and Rockets,* Vol. 25, Jan.-Feb. 1988, pp. 4-8.

[15]Ericsson, L. E. and Reding, J. P., "Aerodynamic Effects of Bulbous Bases," NASA CR-1339, Aug. 1969.

[16]Murphy, C. H., "Free-Flight Motion of Symmetric Missiles," U. S. Army Ballistic Research Lab., Aberdeen Proving Ground, MD, Rept. 1216, July 1963.

[17]Beyers, M. E., "Technique for Smoothing Free-Flight Oscillation Data," *Journal of Spacecraft and Rockets*, Vol. 12, May 1975, pp. 318-319.

[18]Steinberg, S., Uselton, B. L., and Siemers, P. M., III, "Viking Pitch Damping Derivatives as Influenced by Support Interference and Test Techniques," *Journal of Spacecraft and Rockets*, Vol. 10, July 1973, pp. 443-449.

[19]Ericsson, L. E. and Reding, J. P., "Review of Support Interference in Dynamic Tests," *AIAA Journal*, Vol. 21, Dec. 1983, pp. 1652-1666.

[20]Dayman, B., Jr., "Free Flight Testing in High-Speed Wind Tunnels," AGARDograph 113, May 1966.

[21]Beyers, M. E., "Investigation of High-Maneuverability Flight Vehicle Dynamics," International Council of the Aeronautical Sciences, Paper 80-7.2, Oct. 1980.

Walter B. Sturek
Associate Editor